Structural Engineering and Mechanics, *Vol. 57, No. 2 (2016) 201-220*
DOI: http://dx.doi.org/10.12989/sem.2016.57.2.201

Wave propagation in a two-temperature fiber-reinforced magneto-thermoelastic medium with three-phase-lag model

Samia M. Said[*1] and Mohamed I.A. Othman[2]

[1]*Department of Mathematics, Faculty of Science, P.O. Box 44519, Zagazig University, Zagazig, Egypt*
[2]*Department of Mathematics, Faculty of Science, Taif University 888, Saudi Arabia*

(Received June 10, 2015, Revised October 26, 2015, Accepted December 2, 2015)

Abstract. A general model of equations of the two-temperature theory of generalized thermoelasticity is applied to study the wave propagation in a fiber-reinforced magneto-thermoelastic medium in the context of the three-phase-lag model and Green-Naghdi theory without energy dissipation. The material is a homogeneous isotropic elastic half-space. The exact expression of the displacement components, force stresses, thermodynamic temperature and conductive temperature is obtained by using normal mode analysis. The variations of the considered variables with the horizontal distance are illustrated graphically. Comparisons are made with the results of the two theories in the absence and presence of a magnetic field as well as a two-temperature parameter. A comparison is also made between the results of the two theories in the absence and presence of reinforcement.

Keywords: fiber-reinforced; Green-Naghdi theory; three-phase-lag model; magnetic field

1. Introduction

Fiber-reinforced composites are widely used in engineering structures, due to their superiority over the structural materials in applications requiring high strength and stiffness in lightweight components. A continuum model is used to explain the mechanical properties of such materials. A reinforced concrete member should be designed for all conditions of stresses that may occur and in accordance with the principles of mechanics. The characteristic property of a reinforced concrete member is that its components, namely concrete and steel, act together as a single unit as long as they remain in the elastic condition, i.e., the two components are bound together so that there can be no relative displacement between them. In the case of an elastic solid reinforced by a series of parallel fibers, it is usual to assume transverse isotropy. In the linear case, the associated constitutive relations, relating infinitesimal stress and strain components have five material constants. In the last three decades, the analysis of stress and deformation of fiber-reinforced composite materials has been an important research area of solid mechanics. The wave propagation in a reinforced medium plays a very interesting role in civil engineering and geophysics. The studies of propagation, reflection, and transmission of waves are of great interest

∗Corresponding author, Ph.D. Student, E-mail: Samia_said59@yahoo.com
[a]Professor, E-mail: m_i_a_othman@yahoo.com

http://www.techno-press.org/?journal=sem&subpage=8 ISSN: 1225-4568 (Print), 1598-6217 (Online)

to seismologists. Such studies help them to obtain knowledge about the rock structures as well as their elastic properties and at the same time information regarding minerals and fluids present inside the earth. Belfield *et al*. (1983) introduced the idea of a continuous self-reinforcement at every point of an elastic solid. One can find some studies on transversely isotropic elasticity in the literature by, Singh and Singh (2004), Singh (2006), Abbas *et al*. (2011, 2012, 2014), Othman *et al*. (2012a, b, 2013, 2015), Abd-Alla *et al*. (2015).

A theory of heat conduction in deformable bodies which depends upon two distinct temperatures, the conductive temperature and the thermodynamic temperature, has been established by Chen and Gurtin (1968), Chen *et al*. (1968, 1969). In time-independent problems, the difference between these two distinct temperatures is proportional to the heat supply and in the absence of any heat supply; these two temperatures are identical as Chen *et al*. (1968). In time-dependent situations and of the wave propagation problems, in particular, the two-temperatures are in general different, regardless of the presence of a heat supply. Warren and Chen (1973) have studied the wave propagation in the two-temperature theory of thermoelasticity. Youssef (2005) has proposed a theory in the context of the generalized theory of thermoelasticity with two-temperature. The propagation of harmonic plane waves in the media described by the two-temperature theory of thermoelasticity is investigated by Puri and Jordan (2005). Several problems have been solved by Kumar and Mukhopadhyay (2010), Das and Kanoria (2012), Othman *et al*. (2014), Zenkour and Abouelregal (2015) applying the two-temperature theory of thermoelasticity.

It is well known that the usual theory of heat conduction based on Fourier's law predicts an infinite heat propagation speed. It is also known that heat transmission at low temperature propagates by means of waves. These aspects have caused intense activity in the field of heat propagation. Extensive reviews on the second sound theories (hyperbolic heat conduction) are given in Hetnarski and Ignaczak (1999, 2000). A two-phase-lag to both the heat flux vector and the temperature gradient was introduced by Tzou (1995). According to this model, classical Fourier's law $\boldsymbol{q}=-K\nabla T$ has been replaced by $\boldsymbol{q}\ (P,\ t+\tau q)=-K\nabla T(P,\ t+\tau_T)$, where the temperature gradient ∇T at a point P of the material at time $t+\tau_T$ corresponds to the heat flux vector $\boldsymbol{q}$ at the same point at time $t+\tau q$. Here K is the thermal conductivity of the material. The delay time τ_T is interpreted as that caused by the micro-structural interactions and is called the phase-lag of the temperature gradient. The other delay time τq is interpreted as the relaxation time due to the fast transient effects of thermal inertia and is called the phase-lag of the heat flux. Recently, Roy Choudhuri (2007) has proposed a theory with three-phase lag (3PHL) which is able to contain all the previous theories at the same time. In this case Fourier's law $\boldsymbol{q}=-K\nabla T$ has been replaced by $\boldsymbol{q}\ (P,\ t+\tau_q)=-[K\nabla T(P,\ t+\tau_T)+K^*\nabla v(P,\ t+\tau_v)]$, where $\nabla v(\dot{v}=T)$ is the thermal displacement gradient, K^* is the additional material constant and τ_v is the phase-lag for the thermal displacement gradient. The purpose of the work of Roy Choudhuri (2007) was to establish a mathematical model that includes (3PHL) in the heat flux vector, the temperature gradient and in the thermal displacement gradient. For this model, we can consider several kinds of Taylor approximations to recover the previously cited theories. In particular the thermoelasticity without energy dissipation (TEWOED) and thermoelasticity with energy dissipation (TEWED) introduced by Green and Naghdi (1991, 1992, 1993) are recovered. A three-phase-lag model is very useful in the problems of nuclear boiling, exothermic catalytic reactions, phonon-electron interactions, phonon-scattering etc. Quintanilla and Racke (2008), Quintanilla (2009), Kumar *et al*. (2012), Abbas (2014), Kumar and Kumar (2015) have solved different problems applying the (3PHL) model.

The investigation of interaction between a magnetic field, stress, and strain in a thermoelastic solid is very important due to its many applications in diverse field such as geophysics (for understanding the effect of the Earth's magnetic field on seismic waves), damping of acoustic waves in a magnetic field, designing machine elements like heat exchangers, boiler tubes (where the temperature induced elastic deformation occurs), biomedical engineering (problems involving thermal stress), emissions of the electromagnetic radiations from nuclear devices, development of a highly sensitive super conducting magnetometer, electrical power engineering, plasma physics, etc. Many studies in a generalized magneto-thermoelasticity can be found in the literatures by Abbas and Youssef (2009), Othman *et al.* (2008, 2009, 2011, 2015).

Our main object in writing this paper is to present a two-temperature fiber-reinforced magneto-thermoelastic medium due to the thermal shock in the context of the three-phase-lag (3PHL) model and the thermoelasticity without energy dissipation (G-N II) theory. The governing equations of the problem are solved by using normal mode analysis. The effect of a magnetic field, a two-temperature parameter and reinforcement on the physical quantities is also studied.

2. Formulation of the problem and basic equations

We consider the problem of a thermoelastic half-space ($x \geq 0$). A magnetic field with a constant intensity $H=(0,0,H_0)$, is acting parallel to the boundary plane (taken as the direction of the z-axis). The surface of a half-space is subjected to a thermal shock which is a function of y and t. We are interested in a plane strain in the xy-plane with displacement vector $\boldsymbol{u}=(u,v,0)$. We begin our consideration with linearized electromagnetism equations as Othman and Said (2015)

$$\boldsymbol{J} = \nabla \wedge \boldsymbol{h} - \varepsilon_0 \frac{\partial \boldsymbol{E}}{\partial t} \tag{1}$$

$$\nabla \wedge \boldsymbol{E} = -\mu_0 \frac{\partial \boldsymbol{h}}{\partial t} \tag{2}$$

$$\boldsymbol{E} = -\mu_0 (\dot{\boldsymbol{u}} \wedge \boldsymbol{H}) \tag{3}$$

$$\nabla . \boldsymbol{h} = 0 \tag{4}$$

where μ_0 is the magnetic permeability, ε_0 is the electric permeability, $\boldsymbol{J}$ is the current density vector, $\dot{\boldsymbol{u}}$ is the particle velocity of the medium, and the small effect of the temperature gradient on $\boldsymbol{J}$ is also ignored. These equations, supplemented by the field equations and constitutive relations for a fiber-reinforced linearly thermoelastic isotropic medium with respect to the reinforcement direction $\boldsymbol{a}$ in the (3PHL) model without body forces, body couples and heat sources

(i) The stress-strain relation may be written as Belfield *et al.* (1983)

$$\sigma_{ij} = \lambda e_{kk}\delta_{ij} + 2\mu_T e_{ij} + \alpha(a_k a_m e_{km}\delta_{ij} + a_i a_j e_{kk}) + 2(\mu_L - \mu_T)(a_i a_k e_{kj} + a_j a_k e_{ki}) + \beta a_k a_m e_{km} a_i a_j - \gamma \hat{T}\delta_{ij}, \tag{5}$$

where σ_{ij}'s are the components of stress, e_{ij}'s are the components of strain, e_{kk} is the dilatation, λ, μ_T's are the elastic constants, α, β, γ, $(\mu_L - \mu_T)$ are reinforcement parameters, δ_{ij} is the Kronecker delta, $\hat{T} = T - T_0$ where T is the temperature above the reference temperature T_0, and $\boldsymbol{a} \equiv (a_1, a_2, a_3)$, $a_1^2 + a_2^2 + a_3^2 = 1$. We choose the fiber direction as $\boldsymbol{a} \equiv (1, 0, 0)$. The strains can be expressed in terms of the displacement u_i as

$$e_{ij} = \frac{1}{2}(u_{i,j} + u_{j,i}), \quad e_{kk} = e = \frac{\partial u}{\partial x} + \frac{\partial v}{\partial y}, \quad i, j = x, y. \tag{6}$$

Eq. (5) then yields

$$\sigma_{xx} = A_{11}u_{,x} + A_{12}v_{,y} - \gamma\hat{T} \tag{7}$$

$$\sigma_{yy} = A_{12}u_{,x} + A_{22}v_{,y} - \gamma\hat{T} \tag{8}$$

$$\sigma_{xy} = \mu_L(u_{,y} + v_{,x}), \quad \sigma_{xz} = \sigma_{yz} = 0, \tag{9}$$

where $A_{11}=\lambda+2(\alpha+\mu_T)+4(\mu_L-\mu_T)+\beta$, $A_{12}=\lambda+\alpha$, $A_{22}=\lambda+2\mu_T$.

(ii) The equation of motion, taking into consideration the Lorentz force, is given by

$$\rho\,\ddot{u}_i = \sigma_{ij,j} + \mu_0(\boldsymbol{J}\wedge\boldsymbol{H})_i, \qquad i, j = 1, 2, 3. \tag{10}$$

The dynamic displacement vector is actually measured from a steady-state deformed position and the deformations are assumed to be small. Due to the application of the initial magnetic field $\boldsymbol{H}$, there are an induced magnetic field $\boldsymbol{h}$=(0,0,h) and an induced electric field $\boldsymbol{E}$, as well as the simplified equations of electrodynamics of a slowly moving medium for a homogeneous, thermal and electrically conducting, elastic solid. Expressing the components of the vector $\boldsymbol{J}$=(J_1, J_2, J_3) in terms of displacement by eliminating the quantities $\boldsymbol{h}$ and $\boldsymbol{E}$, from Eq. (1), thus yields

$$J_1 = H_0\left(-\frac{\partial e}{\partial y} + \mu_0\,\varepsilon_0\,\ddot{v}\right), \quad J_2 = H_0\left(\frac{\partial e}{\partial x} - \mu_0\,\varepsilon_0\,\ddot{u}\right), \quad J_3 = 0 \tag{11}$$

where $h=-H_0 e$.

By substituting from Eqs. (7)-(9) and (11) in Eq. (10) and using the summation convection: we note that the third equation of motion in Eq. (10) is identically satisfied and the first two equations become

$$\rho\frac{\partial^2 u}{\partial t^2} = A_{11}\frac{\partial^2 u}{\partial x^2} + B_2\frac{\partial^2 v}{\partial x \partial y} + B_1\frac{\partial^2 u}{\partial y^2} - \gamma\frac{\partial \hat{T}}{\partial x} - \mu_0 H_0\frac{\partial h}{\partial x} - \varepsilon_0\mu_0^2 H_0^2\frac{\partial^2 u}{\partial t^2} \tag{12}$$

$$\rho\frac{\partial^2 v}{\partial t^2} = A_{22}\frac{\partial^2 v}{\partial y^2} + B_2\frac{\partial^2 u}{\partial x \partial y} + B_1\frac{\partial^2 v}{\partial x^2} - \gamma\frac{\partial \hat{T}}{\partial y} - \mu_0 H_0\frac{\partial h}{\partial y} - \varepsilon_0\mu_0^2 H_0^2\frac{\partial^2 v}{\partial t^2} \tag{13}$$

where $B_1=\mu_L$, $B_2=A_{12}+\mu_L$.

(iii) The generalized heat conduction equation in the context of the (3PHL) model with two-temperature is given by Youssef (2005), Roy Choudhuri (2007)

$$K^*\nabla^2\Phi + \tau_v^*\nabla^2\dot{\Phi} + K\tau_T\nabla^2\ddot{\Phi} = \left(1 + \tau_q\frac{\partial}{\partial t} + \frac{1}{2}\tau_q^2\frac{\partial^2}{\partial t^2}\right)(\rho\,C_E\ddot{T} + \gamma\,T_0\ddot{e}). \tag{14}$$

The relation between the conductive temperature and the thermodynamic temperature is

$$\Phi - T = \delta\,\Phi_{,ii}, \tag{15}$$

where K^* is the additional material constant, K is the coefficient of thermal conductivity, ρ is the mass density, C_E is the specific heat at constant strain, Φ is the conductive temperature, δ>0 a constant called two-temperature parameter, τ_T and τ_q are the phase-lag of temperature gradient and the phase-lag of heat flux respectively. Also $\tau_v^* = K + \tau_v K^*$, where τ_v is the phase-lag of thermal displacement gradient. Eqs. (12)-(14), when $K=\tau_T=\tau_q=\tau_v=0$, reduce to the equations of the (GN-II) theory. In the above equations a dot denotes partial derivative with respect to time, and a comma followed by a suffix denotes partial derivative with respect to the corresponding coordinates. Introducing the following non-dimensions quantities

$$(x',y',u',v')=c_1\eta(x,y,u,v),\ \ (t',\tau_q',\tau_v',\tau_T')=c_1^2\eta(t,\tau_q,\tau_v,\tau_T),\ \ h'=\frac{h}{H_0},\ \ \theta=\frac{\gamma\hat{T}}{(\lambda+2\mu_T)},$$

$$\sigma_{ij}'=\frac{\sigma_{ij}}{\mu_T},\ \ \Phi'=\frac{\gamma(\Phi-T_0)}{(\lambda+2\mu_T)},\ \ \eta=\frac{\rho C_E}{K^*},\ \ c_1^2=\frac{(\lambda+2\mu_T)}{\rho}. \tag{16}$$

Using the above non-dimension variables defined in Eq. (16) then employing $h'=-H_0e$, the above governing equations takes the following form (dropping the primes for convenience)

$$\alpha_0\frac{\partial^2 u}{\partial t^2}=L_{11}\frac{\partial^2 u}{\partial x^2}+L_2\frac{\partial^2 v}{\partial x\,\partial y}+h_1\frac{\partial^2 u}{\partial y^2}-\frac{\partial\theta}{\partial x}, \tag{17}$$

$$\alpha_0\frac{\partial^2 v}{\partial t^2}=L_{22}\frac{\partial^2 v}{\partial y^2}+L_2\frac{\partial^2 u}{\partial x\,\partial y}+h_1\frac{\partial^2 v}{\partial x^2}-\frac{\partial\theta}{\partial y}, \tag{18}$$

$$C_K\Phi_{,ii}+C_v\dot{\Phi}_{,ii}+C_T\ddot{\Phi}_{,ii}=(1+\tau_q\frac{\partial}{\partial t}+\frac{1}{2}\tau_q^2\frac{\partial^2}{\partial t^2})(\ddot{\theta}+\varepsilon\ddot{e}), \tag{19}$$

$$\Phi-\theta=\beta_0\Phi_{,ii}, \tag{20}$$

where, $L_{11}=h_{11}+h_0H_0,\ \ L_{22}=h_{22}+h_0H_0,\ \ L_2=h_2+h_0H_0,\ \ h_0=\dfrac{\mu_0H_0^2}{\rho c_1^2},\ \ C_K=\dfrac{K^*}{\rho C_E c_1^2},\ \ C_T=\dfrac{\eta K\tau_T}{\rho C_E},$

$$(h_1,h_2,h_{11},h_{22})=\frac{(B_1,B_2,A_{11},A_{22})}{\rho c_1^2},\ \ C_v=\frac{\eta K}{\rho C_E}+C_K\tau_v,\ \ \varepsilon=\frac{\gamma^2 T_0}{\rho C_E(\lambda+2\mu_T)},\ \ \beta_0=\delta c_1^2\eta^2,\ \ \alpha_0=1+\frac{\varepsilon_0\mu_0^2H_0^2}{\rho}.$$

3. Normal mode analysis

The solution of the considered physical variable can be decomposed in terms of normal mode as the following form

$$[u,v,\theta,\Phi,\sigma_{ij}](x,y,t)=[u^*,v^*,\theta^*,\Phi^*,\sigma_{ij}^*](x)\exp(\omega t+\mathrm{i}my), \tag{21}$$

where ω is a complex constant, $\mathrm{i}=\sqrt{-1}$, m is the wave number in the y-direction, and $u^*(x)$, $v^*(x)$, $\theta^*(x)$, $\Phi^*(x)$, $\sigma_{ij}^*(x)$ are the amplitudes of the field quantities.

Introducing from Eq. (21) in Eqs. (17)-(20), we get

$$[L_{11}\mathrm{D}^2-N_1]u^*+\mathrm{i}mL_2\mathrm{D}v^*=\mathrm{D}\theta^*, \tag{22}$$

$$\mathrm{i}mL_2\mathrm{D}u^*+[h_1\mathrm{D}^2-N_2]v^*=\mathrm{i}m\,\theta^*, \tag{23}$$

$$\varepsilon N_3\mathrm{D}u^*+\mathrm{i}\varepsilon mN_3v^*+N_3\theta^*=[N_4\mathrm{D}^2-N_5]\Phi^*, \tag{24}$$

$$\theta^*=(N_8-\beta_0\mathrm{D}^2)\Phi^*, \tag{25}$$

where, $N_1 = \alpha_0\omega^2 + h_1 m^2$, $N_2 = \alpha_0\omega^2 + L_{22} m^2$, $N_3 = \omega^2(1+\tau_q\omega+\frac{1}{2}\tau_q^2\omega^2)$, $N_4 = C_K + C_v\omega + C_T\omega^2$, $N_5 = N_4 m^2$, $N_8 = 1+\beta_0 m^2$.

Introducing Eq. (25) in Eqs. (22)-(24), thus we have

$$[L_{11}\mathrm{D}^2 - N_1]u^* + \mathrm{i}\, mL_2\mathrm{D}v^* = \mathrm{D}(N_8 - \beta_0\mathrm{D}^2)\Phi^*, \tag{26}$$

$$\mathrm{i}\, mL_2\mathrm{D}\,u^* + [h_1\mathrm{D}^2 - N_2]v^* = \mathrm{i}\, m\,(N_8 - \beta_0\mathrm{D}^2)\,\Phi^*, \tag{27}$$

$$\varepsilon N_3\mathrm{D}u^* + \mathrm{i}\varepsilon\, mN_3\, v^* = [N_6\mathrm{D}^2 - N_7]\Phi^*, \tag{28}$$

where $N_6 = N_4 + \beta_0 N_3$, $N_7 = N_5 + N_3 N_8$, $\mathrm{D} = \frac{\mathrm{d}}{\mathrm{d}x}$.

Eliminating $v^*(x)$ and $\Phi^*(x)$ between Eqs. (26)-(28), we obtain the sixth order-ordinary differential equation satisfied with $u^*(x)$

$$[\mathrm{D}^6 - A\,\mathrm{D}^4 + B\,\mathrm{D}^2 - C\,]u^*(x) = 0, \tag{29}$$

where $A = \frac{d_1}{d_4}$, $B = \frac{d_2}{d_4}$, $C = \frac{d_3}{d_4}$,

$$d_1 = N_1N_6h_1 + L_{11}N_2N_6 + h_1N_7L_{11} + m^2\varepsilon N_3\beta_0L_{11} + \varepsilon N_3N_2\beta_0 + \varepsilon N_3N_8h_1 - 2m^2\varepsilon N_3\beta_0 L_2 - m^2L_2^2N_6,$$

$$d_2 = L_{11}N_2N_7 + m^2\varepsilon N_3N_8L_{11} + N_1N_2N_6 + N_1N_7h_1 + \varepsilon N_3N_1\beta_0m^2 + \varepsilon N_3N_8N_2 - 2m^2\varepsilon N_3N_8 L_2 - m^2L_2^2N_7,$$

$$d_3 = N_1N_2N_7 + m^2\,\varepsilon\, N_3N_8N_1,\quad d_4 = (L_{11}N_6 + \varepsilon N_3\beta_0)\,h_1.$$

Eq. (29) can be factored as

$$(\mathrm{D}^2 - k_1^2)(\mathrm{D}^2 - k_2^2)(\mathrm{D}^2 - k_3^2)\,u^*(x) = 0, \tag{30}$$

where k_n^2 $(n = 1, 2, 3)$ are the roots of the characteristic equation of Eq. (29).

The solution of Eq. (29), which is bound as $x\to\infty$, is given by

$$u^*(x) = \sum_{n=1}^{3} G_n \exp(-k_n x). \tag{31}$$

Similarly

$$v^*(x) = \sum_{n=1}^{3} R_{1n}G_n \exp(-k_n x), \tag{32}$$

$$\Phi^*(x) = \sum_{n=1}^{3} R_{2n}G_n \exp(-k_n x), \tag{33}$$

where $R_{1n} = \frac{\mathrm{i}\, m\left(N_1 - (L_{11} - L_2)k_n^2\right)}{h_1k_n^3 - (N_2 - m^2L_2)k_n}$, $R_{2n} = \frac{-N_1 + L_{11}k_n^2 - imL_2k_nR_{1n}}{-N_8k_n + \beta_0k_n^3}$.

Introducing Eq. (33) in Eq. (25), we have

$$\theta^*(x) = \sum_{n=1}^{3} R_{3n}G_n \exp(-k_n x), \tag{34}$$

where, $R_{3n} = (N_8 - \beta_0 k_n^2) R_{2n}$.

Using Eqs. (16) and (21) in Eqs. (7) and (9), we obtain

$$\sigma_{xx}^* = \frac{1}{\mu_T}[A_{11}\mathrm{D}u^* + imA_{12}v^* - (\lambda + 2\mu_T)\theta^*], \tag{35}$$

$$\sigma_{xy}^* = \frac{\mu_L}{\mu_T}[imu^* + \mathrm{D}v^*]. \tag{36}$$

Introducing Eqs. (31), (32) and (34) in Eqs. (35) and (36), this yields

$$\sigma_{xx}^*(x) = \sum_{n=1}^{3} R_{4n} G_n \exp(-k_n x), \tag{37}$$

$$\sigma_{xy}^* = \sum_{n=1}^{3} R_{5n}\, G_n\, \exp(-k_n x), \tag{38}$$

where $R_{4n} = \frac{1}{\mu_T}[-A_{11}k_n + imA_{12}R_{1n} - (\lambda + 2\mu_T)R_{3n}]$, $R_{5n} = \frac{\mu_L}{\mu_T}(\mathrm{i}m - k_n R_{1n})$.

4. Boundary conditions

We consider the problem of a two-temperature fiber-reinforced thermoelastic medium under the effect of a magnetic field which fills the region Ω defined as follows:

$$\Omega = \{(x, y, z) : 0 \le x < \infty, -\infty < y < \infty, -\infty < z < \infty\}.$$

In the physical problem, we should suppress the positive exponentials that are unbounded at infinity. In order to determine the parameters G_n (n=1,2,3), we need to consider the boundary conditions at x=0 as follows:

(i) A thermal boundary condition that the surface of the half-space is subjected to an isothermal boundary

$$\theta(0, y, t) = 0, \tag{39}$$

(ii) A mechanical boundary condition that the surface of the half-space is subjected to mechanical force

$$\sigma_{xx} = f(0, y, t) = -f^* \exp(\omega t + \mathrm{i}my), \tag{40}$$

(iii) A mechanical boundary condition that the surface of the half-space is traction free

$$\sigma_{xy}(0, y, t) = 0, \tag{41}$$

$f(y,t)$ is an arbitrary function of y, t and f^* is a constant. Substituting the expressions of the variables considered into the above boundary conditions Eqs. (39)-(41), we can obtain the following equations satisfied by the parameters

$$\sum_{n=1}^{3} R_{3n} G_n = 0, \quad \sum_{n=1}^{3} R_{4n} G_n = -f^*, \quad \sum_{n=1}^{3} R_{5n} G_n = 0 \tag{42}$$

Solving the above system of Eq. (42), we obtain a system of three equations. After applying the inverse of matrix method, we have the values of the three constants G_n (n=1,2,3). Hence, we obtain the expressions of displacements, the thermodynamic temperature, the conductive temperature and the stress components.

$$\begin{pmatrix} G_1 \\ G_2 \\ G_3 \end{pmatrix} = \begin{pmatrix} R_{31} & R_{32} & R_{23} \\ R_{41} & R_{42} & R_{43} \\ R_{51} & R_{52} & R_{53} \end{pmatrix}^{-1} \begin{pmatrix} 0 \\ -f^* \\ 0 \end{pmatrix} \tag{43}$$

5. Numerical calculation and discussion

In order to illustrate the theoretical results obtained in the preceding section and to compare these in the context of the (3PHL) model and the (GN-II) theory, we now present some numerical results for the physical constants as

$$\lambda = 9.59\text{x}10^8\ \text{N.m}^{-2},\ \mu_T = 1.89\text{x}10^9\ \text{N.m}^{-2},\ \mu_L = 2.45\text{x}10^9\ \text{N.m}^{-2},\ \rho = 7800\text{kg.m}^{-3},\ m = 1.2,\ f^* = 0.1,$$

$$\alpha = -1.28\ \text{x}10^9\ \text{N.m}^{-2},\ \beta = 0.32\ \text{x}10^9\ \text{N.m}^{-2},\ C_E = 383.1\ \text{J.kg}^{-1}.\text{K}^{-1},\ \tau_T = 0.007\,\text{s},\ \tau_q = 0.009\,\text{s},$$

$$K^* = 386\ \text{W.m}^{-1}.\text{K}^{-1}.\text{s}^{-1},\ \mu = 1.86\text{x}10^8\ \text{kg.m}^{-1}.\text{s}^{-2},\ K = 800\ \text{W.m}^{-1}.\text{K}^{-1},\quad \omega = \omega_0 + i\xi,\quad \omega_0 = -0.2,$$

$$\delta = 12,\ \ \alpha_t = 3.78\ \text{x}10^{-3}\ \text{K}^{-1},\ \tau_v = 0.006\text{s},\ T_0 = 293\text{K},\quad H_0 = 100,\ \varepsilon_0 = 0.3,\ \ \mu_0 = 1.9;\ \ \xi = 0.9\,.$$

The computations were carried out for a value of time t=0.03. The variations of the thermodynamic temperature θ, the conductive temperature Φ, the displacement components u,v and the stress components σ_{xx} and σ_{xy} with distance x in the plane y=−0.9 for the problem under consideration based on the (3PHL) model and the (G-N II) theory were considered. The results are shown in Figs. 1-18. The graphs show four curves predicted by the two different theories of thermoelasticity. In these figures, the solid lines represent the solution in the (3PHL) model and the dashed lines represent the solution derived using the (G-N II) theory. Here all the variables are taken in non-dimensional forms and we consider the five cases

(i) The corresponding equations for a two-temperature fiber-reinforced generalized thermoelastic medium in the absence of the magnetic field from the above mentioned cases by taking H_0=0.

(ii) The corresponding equations for one-temperature fiber-reinforced generalized magneto thermoelastic medium from the above mentioned cases by taking δ to vanish.

(iii) The corresponding equations for a two-temperature generalized thermoelastic medium by taking α, β, (μ_L−μ_T) to vanish.

(iv) Equations of the (3PHL) model when, K, τ_T, τ_q, τ_v>0 and the solutions are always (exponentially) stable if $\frac{2K\tau_T}{\tau_q} > \tau_v^* > K^*\tau_q$ as in Quintanilla and Racke (2008).

(v) Equations of the (GN-II) theory when, K=τ_T=τ_q=τ_v=0

Figs. 1-6 show comparisons between the displacement components u,v the thermodynamic temperature θ the conductive temperature Φ, and the stress components σ_{xx}, σ_{xy} in the absence (α_0=1) and presence (α_0=2.4) of a magnetic field with a two-temperature parameter δ=12.

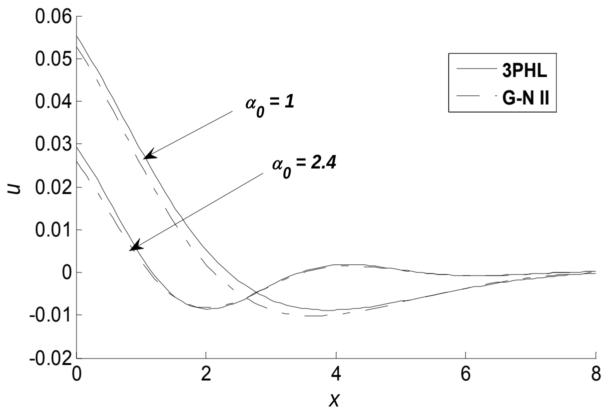

Fig. 1 Horizontal displacement distribution u in the absence and presence of a magnetic field

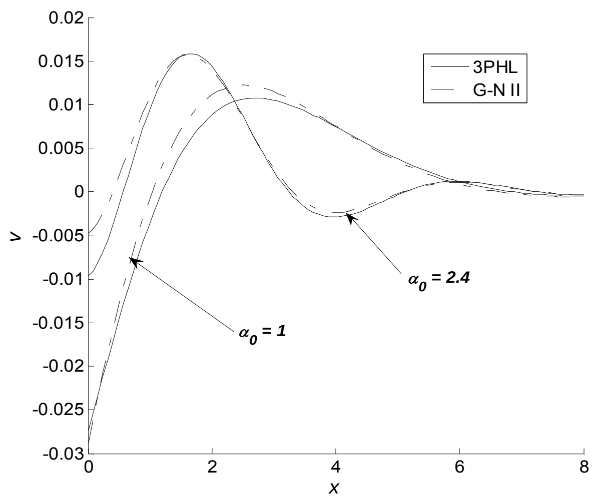

Fig. 2 Vertical displacement distribution v in the absence and presence of a magnetic field

Fig. 1 depicts that the distribution of the horizontal displacement u begins from positive values. In the context of the two theories, u begins with decreasing to a minimum value in the range $0 \le x \le 2$, then increases, and again decreases for α_0=2.4. However, in the context of the two theories, u begins with decreasing to a minimum value in the range $0 \le x \le 4$, and then increases for α_0=1. The magnetic field decreases the magnitude of u in the range $0 \le x \le 2.7$, then increases it. Fig. 2 shows that the distribution of the vertical displacement v begins from negative values. In the context of the two theories, v begins with increasing to a maximum value in the range $0 \le x \le 1.8$. then decreases, again increases, and in the last decreases for α_0=2.4. However, in the context of the two theories, v begins with increasing to a maximum value in the range $0 \le x \le 2.2$, and then decreases for α_0=1. The magnetic field increases the magnitude of v in the range $0 \le x \le 2.2$, then decreases it. The displacements u and v show different behaviors, because of the elasticity of the solid tends to resist a vertical displacement in the problem under the investigation. Fig. 3 exhibits the distribution of the conductive temperature Φ and demonstrates that it begins from negative

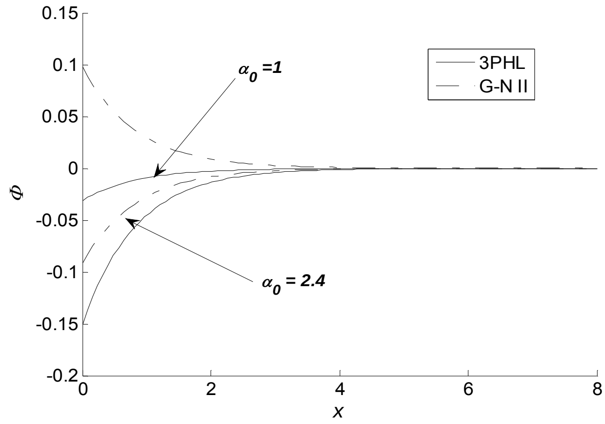

Fig. 3 Conductive temperature distribution Φ in the absence and presence of a magnetic field

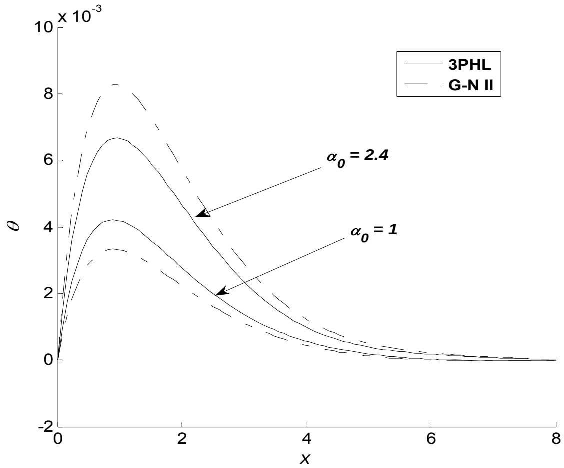

Fig. 4 Thermodynamic temperature distribution θ in the absence and presence of a magnetic field

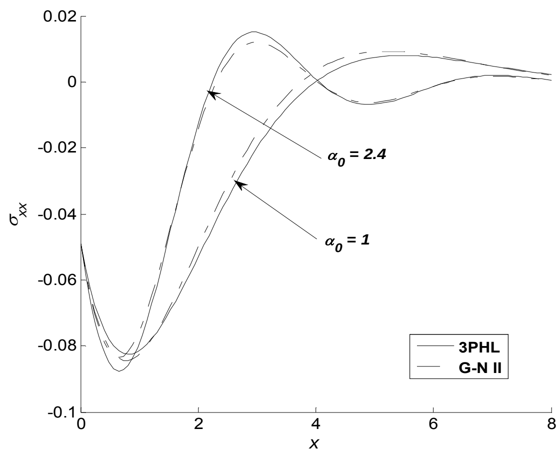

Fig. 5 Distribution of the stress component σ_{xx} in the absence and presence of a magnetic field

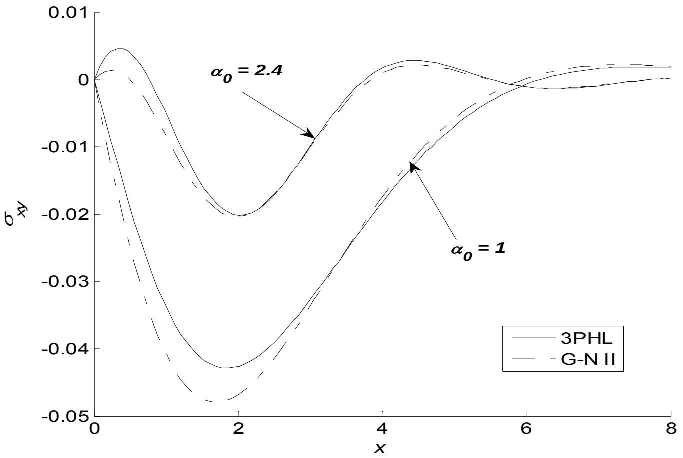

Fig. 6 Distribution of the stress component σ_{xy} in the absence and presence of a magnetic field

values except in the context of the (G-N II) theory for α_0=1, it begins from a positive value. Φ begins with increasing in the range $0 \leq x \leq 4$, and then becomes nearly constant except in the context of the (G-N II) theory for α_0=1, Φ begins with decreasing in the range $0 \leq x \leq 4$, and then becomes nearly constant . The magnetic field decreases the magnitude of Φ. Fig. 4 depicts the distribution of the thermodynamic temperature θ and demonstrates that it reaches a zero value and satisfies the boundary condition at x=0. In the context of the two theories, θ begins with increasing to a maximum value, and then decreases for α_0=1, 2.4. The magnetic field increases the magnitude of θ. Fig. 5 explains that the distribution of the stress component σ_{xx} begins from a negative value and satisfies the boundary condition at x=0. In the context of the two theories, σ_{xx} begins with decreasing to a minimum value in the range $0 \leq x \leq 1$, then increases to a maximum value, and again decreases for α_0=1. However, in the context of the two theories, σ_{xx} decreases to a minimum value in the range $0 \leq x \leq 0.8$, then increases to a maximum value, and also moves in the wave propagation for α_0=2.4. The magnetic field decreases the magnitude of σ_{xx} in the range $0 \leq x \leq 1$, then increases, and again decreases it. Fig. 6 depicts the distribution of the stress component σ_{xy} and demonstrates that it reaches a zero value and satisfies the boundary condition at x=0. The fluctuations of stress component σ_{xy} is x=0. In the context of the two theories, σ_{xy} begins with increasing to a maximum value, then decreases to a minimum value, and also moves in the wave propagation for α_0=2.4. However, in the context of the two theories, σ_{xy} decreases to a minimum, and then increases to a maximum value for α_0=1. The magnetic field increases the magnitude of σ_{xy} in the range $0 \leq x \leq 5.7$, and then decreases it. Figs. 1-6 demonstrate that a magnetic field has a significant role on all the physical quantities. The values of all the physical quantities converge to zero by increasing the distance x; the behavior of two theories are similar. These trends obey elastic and thermoelastic properties of the solid.

Figs. 7-12 show comparisons between the displacement components u, v, the thermo-dynamic temperature θ, the conductive temperature Φ, and the stress components σ_{xx}, σ_{xy} with (δ=12) and without (δ=0) two-temperature parameter in the presence of a magnetic field (α_0=2.4).

Fig. 7 explains that the distribution of the horizontal displacement u begins from positive values in the context of two theories except in the context of the (3PHL) model for δ=0 it begins from a negative value. In the context of the (3PHL) model, u begins with decreasing to a minimum

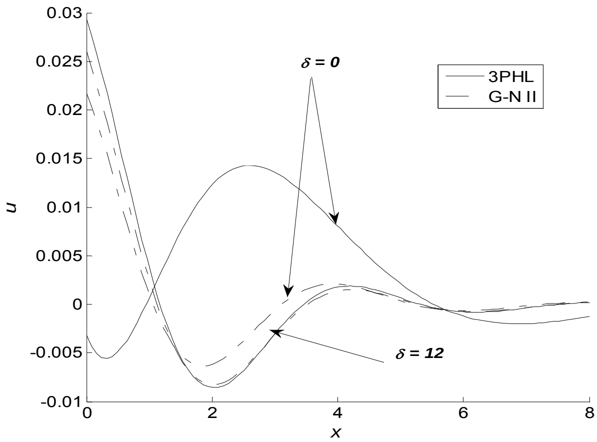

Fig. 7 Horizontal displacement distribution u with and without two-temperature

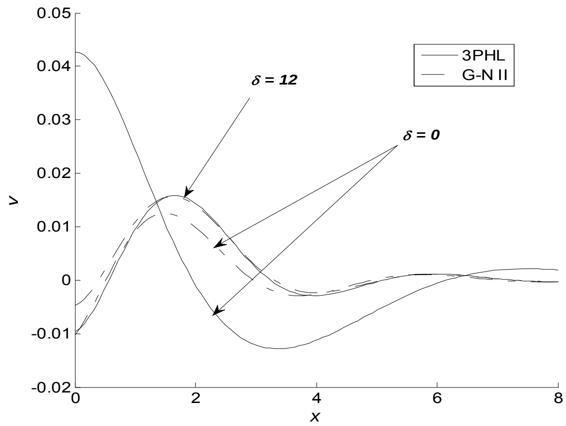

Fig. 8 Vertical displacement distribution v with and without two-temperature

value, then increases to a maximum value, and again decreases for δ=0. However, in the context of the (G-N II) theory, u begins with decreasing to a minimum value in the range $0 \leq x \leq 2$, then increases, again decreases, and in the last increases for δ=0. Fig. 8 exhibits that the distribution of the vertical displacement v begins from negative values in the context of two theories except in the context of the (3PHL) model for δ=0 it begins from a positive value. In the context of the (3PHL) model, u begins with decreasing to a minimum value, and then increases for δ=0. However, in the context of the (G-N II) theory, u begins with increasing to a maximum value, then decreases, again increases, and in the last decreases for δ=0. Fig. 9 shows that the distribution of the conductive temperature Φ begins from negative values for δ=12, but it begins from a zero value for δ=0. In the context of the (3PHL) model, Φ begins with increasing to a maximum value, then decreases to a minimum value, and again increases. However, in the context of the (G-N II) theory, Φ is nearly constant. Fig. 10 exhibits the distribution of the thermodynamic temperature θ and demonstrates that it reaches a zero value and satisfies the boundary condition at x=0. In the context of the (3PHL) model for δ=0, θ begins with increasing to a maximum value, then decreases to a

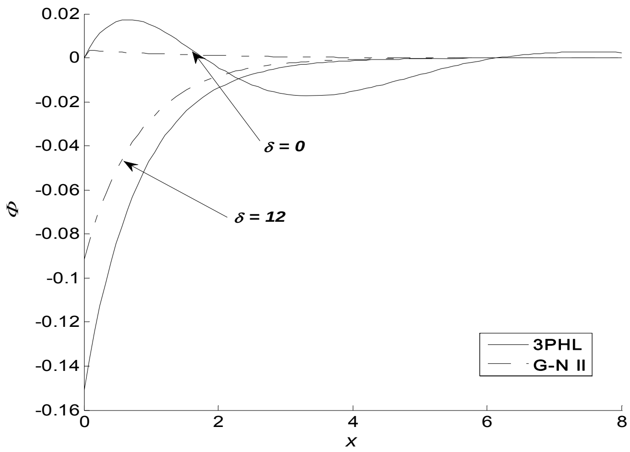

Fig. 9 Conductive temperature distribution Φ with and without two-temperature

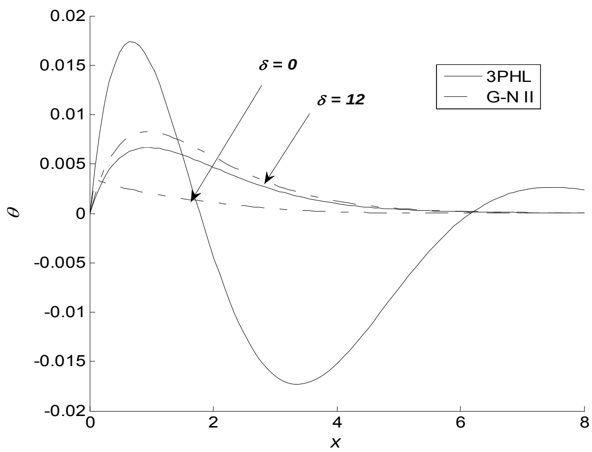

Fig. 10 Thermodynamic temperature distribution θ with and without two-temperature

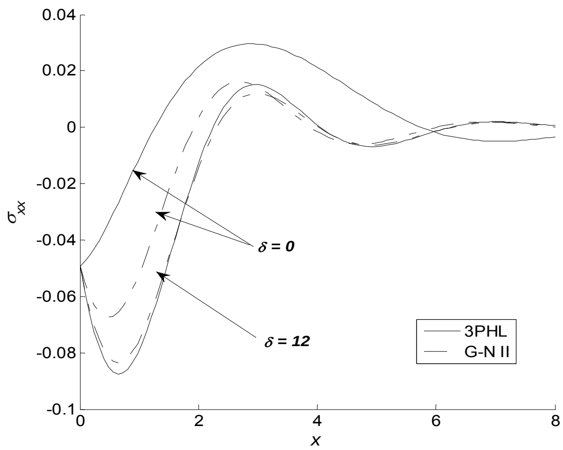

Fig. 11 Distribution of the stress component σ_{xx} with and without two-temperature

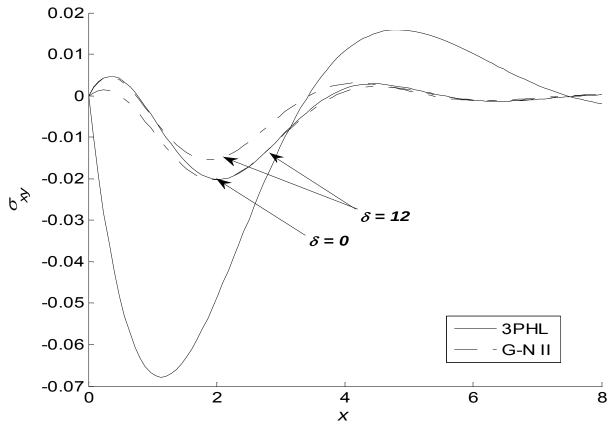

Fig. 12 Distribution of the stress component σ_{xy} with and without two-temperature

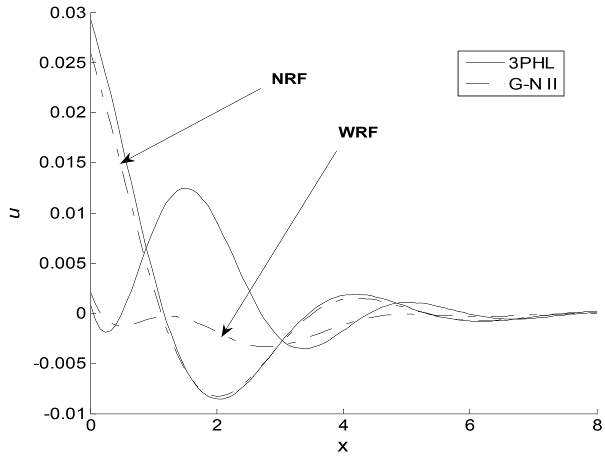

Fig. 13 Horizontal displacement distribution u in the absence and presence of reinforcement

minimum value, and again increases. However, in the context of the (G-N II) theory for δ=0, θ begins with decreasing, and then becomes nearly constant. Fig. 11 explains that the distribution of the stress component σ_{xx} begins from a negative value and satisfies the boundary condition at x=0. In the context of the (3PHL) model, σ_{xx} begins with increases to a maximum value, and then decreases. However, in the context of the (G-N II) theory for δ=0, σ_{xx} begins with decreasing to a minimum value, then increases to a maximum value, and also moves in the wave propagation. Fig. 12 shows the distribution of the stress component σ_{xy} and demonstrates that it reaches a zero value and satisfies the boundary condition at x=0. In the context of the two theories for δ=0, σ_{xy} begins with increasing, then decreases to a minimum value, and also moves in the wave propagation. Figs. 7-12 demonstrate that the two-temperature parameter has a significant role on all the physical quantities. The values of all the physical quantities converge to zero by increasing the distance x; the behavior of the (3PHL) model with one temperature is different.

Figs. 13-18 show comparisons between the displacement components u,v, the thermo-dynamic temperature θ, the conductive temperature Φ, and the stress components σ_{xx}, σ_{xy} in the absence

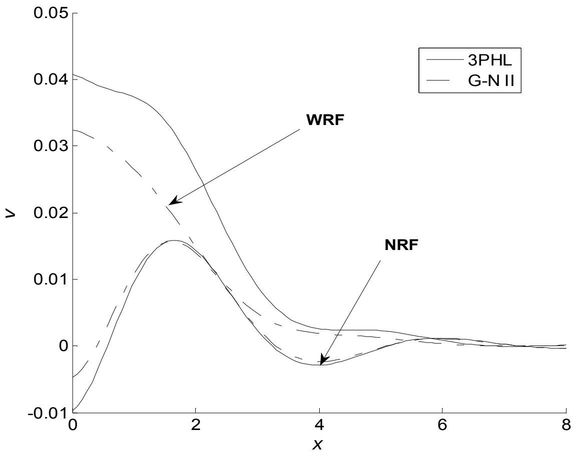

Fig. 14 Vertical displacement distribution v in the absence and presence of reinforcement

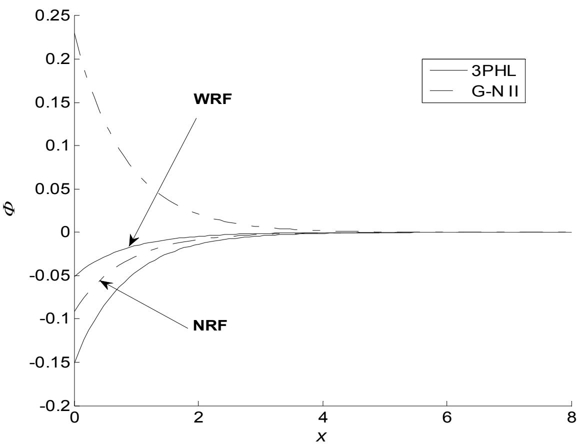

Fig. 15 Conductive temperature distribution Φ in the absence and presence of reinforcement

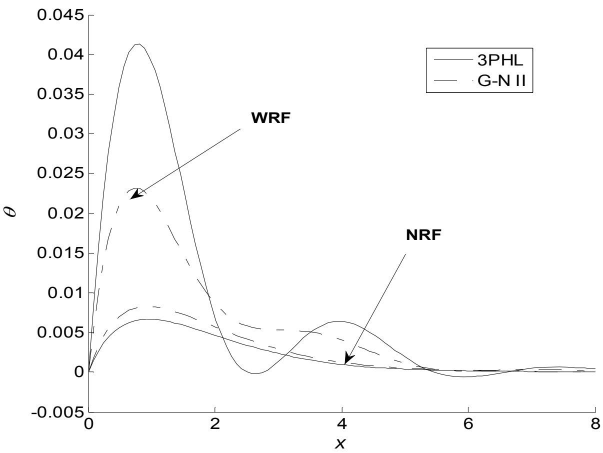

Fig. 16 Thermodyamic temperature distribution θ in the absence and presence of reinforcement

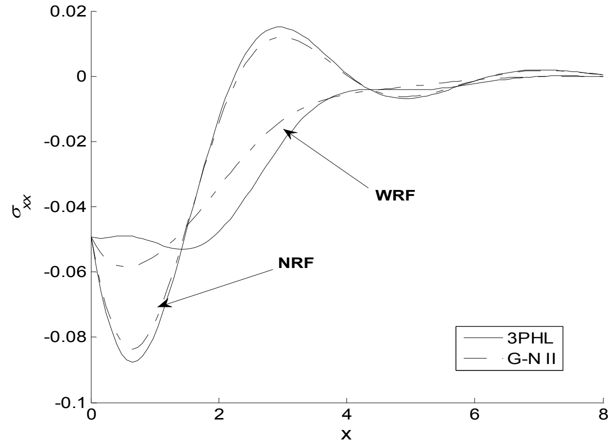

Fig. 17 Distribution of the stress component σ_{xx} in the absence and presence of reinforcement

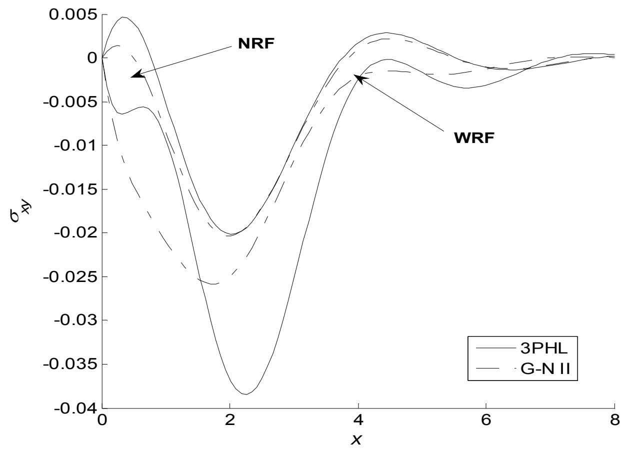

Fig. 18 Distribution of the stress component σ_{xy} in the absence and presence of reinforcement

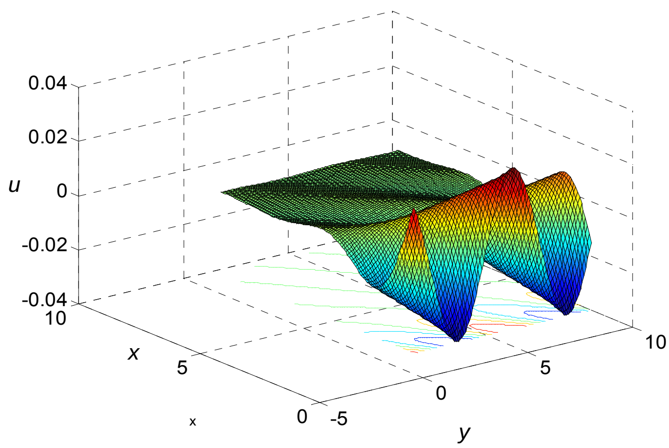

Fig. 19 Horizontal component of displacement against both components of distance based on 3PHL model

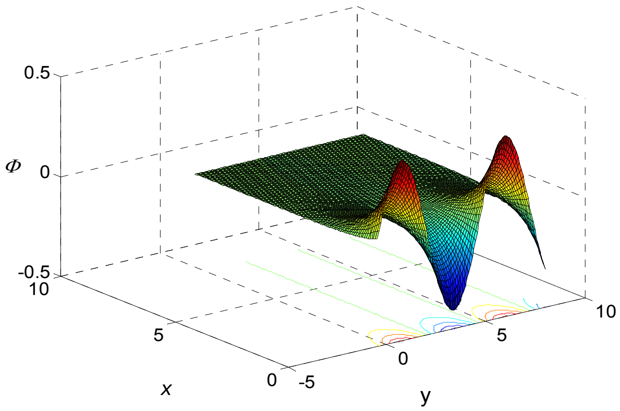

Fig. 20 Conductive temperature distribution Φ against both components of distance based on 3PHL model

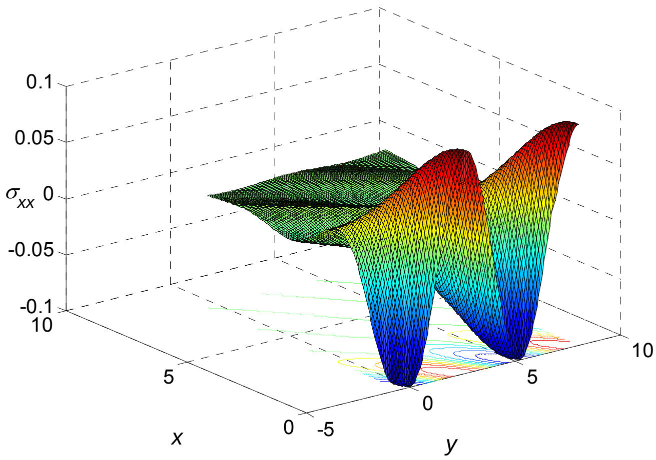

Fig. 21 Distribution of the stress component σ_{xx} against both components of distance based on 3PHL model

(WRF) and presence (NRF) of reinforcement for two-temperature parameter δ=12 and in the presence of a magnetic field (α_0=2.4).

Fig. 13 depicts that the distribution of the horizontal displacement u begins from positive values. In the context of the (3PHL) model, u begins with decreasing, then increases to a maximum value, and also moves in the wave propagation for (WRF). However, in the context of the (G-N II) theory, u begins with decreasing, and then moves in the wave propagation for (WRF). Fig. 14 exhibits that the distribution of the vertical displacement v begins from negative values for (NRF), but it begins from positive values for (WRF). In the context of the two theories, for (WRF) v decreases in the range $0 \le x \le 8$. Fig. 15 shows the distribution of the conductive temperature Φ and demonstrates that it begins from negative values in the context of two theories, but it begins from a positive value in the context of the (G-N II) theory for (WRF). In the context of the (3PHL) model, Φ begins with increasing, and then becomes nearly constant for (WRF). However, in the context of the (G-N II) theory, Φ begins with decreasing, and then becomes nearly constant for (WRF). Fig. 16 exhibits the distribution of the thermodynamic temperature θ and demonstrates that it reaches a zero value and satisfies the boundary condition at x=0. In the context of the two theories, θ begins with increasing to a maximum value, then decreases, and also moves in the wave propagation for (WRF). Fig. 17 shows that the distribution of the stress component σ_{xx} begins from a negative value and satisfies the boundary condition at x=0. In the context of the two theories, σ_{xx} begins with decreasing and then increases for (WRF). Fig. 18 exhibits the distribution of the stress component σ_{xy} and demonstrates that it reaches a zero value and satisfies the boundary condition at x=0. In the context of the two theories, σ_{xy} begins with decreasing to a minimum value, then increases, and also moves in the wave propagation for (WRF). Figs. 13-18 demonstrate that the reinforcement has a significant role on all the physical quantities. All physical quantities begin to coincide when the horizontal distance x increases reach the reference temperature of the solid. These results obey physical reality of the behavior of fiber as a polycrystalline solid.

Figs. 19-21 are giving 3D surface curves for the physical quantities, i.e., the horizontal displacement, the conductive temperature, and the stress components σ_{xx} to study the effect of a magnetic field on the wave propagation within a two-temperature fiber-reinforced thermoelastic isotropic medium in the context of the (3PHL) model. These figures are very important to study the dependence of these physical quantities on the vertical component of distance. The curves obtained are highly depending on the vertical distance from origin, all the physical quantities satisfy boundary condition and are moving in the wave propagation.

5. Conclusions

In the present study, normal mode analysis is applied to study the effect of a magnetic field on the wave propagation in a two-temperature fiber reinforced thermoelastic medium based on the (3PHL) model and the (GN-II) theory. We can obtain the following conclusions based on the above analysis:

- Deformation of a body depends on the nature of the applied force as well as the type of boundary conditions.
- Analytical solution based upon normal mode analysis of the thermoelastic problem in solids have been developed and utilized. Normal mode analysis is, in fact, to look for the solution in Fourier transformed domain, assuming that all the field quantities are sufficiently smooth on the real line such that normal mode analysis of these functions exists.
- The curves in the context of the (3PHL) model and the (GN-II) theory decrease exponentially with increasing this indicates that the thermoelastic waves are un-attenuated and non-dispersive, while purely thermoelastic waves undergo both attenuation and dispersion.
- There are significant differences in the field quantities under the (GN-II) theory and the (3PHL) model due to the phase-lag of temperature gradient and the phase-lag of heat flux.
- The (3PHL) model is useful in the problems of heat transfer, heat conduction, nuclear boiling, exothermic catalytic reactions, phonon-electron interactions, phonon-scattering etc., where the delay time captures the thermal wave behavior (a small scale response in time), the phase-lag captures the effect of phonon-electron interactions (a micro-scopic response in space), the other delay time is effective since, in the (3PHL) model, the thermal displacement gradient is considered as a constitutive variable whereas in the conventional thermoelasticity theory temperature gradient is considered as a constitutive variable.
- It is clear that the magnetic field, the reinforcement and the two-temperature parameter play significant roles on all the physical quantities.

• The vertical distance plays a significant role on all the physical quantities.

References

Abbas, I.A. and Youssef, H.M. (2009), "Finite element method of two-temperature generalized magneto-thermoelasticity," *Arch. Appl. Mech.*, **79**(10), 917-925.

Abbas, I.A. and Abd-Alla, A.N. (2011), "Effect of initial stress on a fiber-reinforced anisotropic thermo-elastic thick plate", *Int. J. Thermophy.*, **32**(5), 1098-1110.

Abbas, I.A. and Othman, M.I.A. (2012), "Generalized thermoelastic interaction in a fiber-reinforced anisotropic half-space under hydrostatic initial stress", *J. Vib. Control*, **18**(2), 175-182.

Abbas, I.A. (2014), "Three-phase lag model on thermoelastic interaction in an unbounded fiber-reinforced anisotropic medium with a cylindrical cavity", *J. Comput. Theor. Nansci.*, **11**(4), 987-992.

Abbas, I.A. and Zenkour, A.M. (2014), "Two-temperature generalized thermoplastic interaction in an infinite fiber-reinforced anisotropic plate containing a circular cavity with two relaxation times", *J. Comput. Theor. Nanosci.*, **11**(1), 1-7.

Abd-Alla, A.M., Abo-Dahab, S.M. and Bayones, F.S. (2015) "Wave propagation in fibre-reinforced anisotropic thermoelastic medium subjected to gravity field", *Struct. Eng. Mech.*, **53**(2), 277-296.

Belfield, A.J., Rogers, T.G. and Spencer, A.J.M. (1983), "Stress in elastic plates reinforced by fibre lying in concentric circles", *J. Mech. Phys. Sol.*, **31**(1), 25-54.

Chen, P.J. and Gurtin, M.E. (1968), "On a theory of heat conduction involving two temperatures", *ZAMP*, **19**(4), 614- 627.

Chen, P.J. and Williams, W.O. (1968), "A note on non simple heat conduction", *ZAMP*, **19**(6), 969-970.

Chen, P.J., Gurtin, M.E. and Williams, W.O. (1969), "On the thermodynamics of non-simple elastic materials with two-temperatures", *ZAMP*, **20**(1), 107-112.

Das, P. and Kanoria, M. (2012), "Two-temperature magneto-thermoelastic response in a perfectly conducting medium based on GN-III model", *Int. J. Pure. Appl. Math.*, **81**(2), 199-229.

Green, A.E. and Naghdi, P.M. (1991), "A re-examination of the basic postulate of thermo- mechanics", *Proc. Roy. Soc. London*, **432**(1885), 171-194.

Green, A.E. and Naghdi, P.M. (1992), "On undamped heat waves in an elastic solid", *J. Therm. Stress.*, **15**(2), 253-264.

Green, A.E. and Naghdi, P.M. (1993), "Thermoelasticity without energy dissipation", *J. Elast.*, **31**(3), 189-208.

Hetnarski, R.B. and Ignaczak, J. (1999), "Generalized thermoelasticity", *J. Therm. Stress.*, **22**(4-5), 451-476.

Hetnarski, R.B. and Ignaczak, J. (2000), "Nonclassical dynamical thermoelasticity", *Int. J. Sol. Struct.*, **37**(1), 215-224.

Kumar, R. and Mukhopadhyay, S. (2010), "Effects of thermal relaxation time on plane wave propagation under two-temperature thermoelasticity", *Int. J. Eng. Sci.*, **48**(2), 128-139.

Kumar, R., Chawla, V. and Abbas, I.A. (2012), "Effect of viscosity on wave propagation in anisotropic thermoelastic medium with three-phase-lag model", *J. Theor. Appl. Mech.*, **39**(4), 313-341.

Kumar, A. and Kumar, R. (2015), "A domain of influence theorem for thermoelasticity with three-phase-lag model", *J. Therm. Stress.*, **38**(7), 744-755.

Othman, M.I.A. and Song, Y. (2008), "Reflection of magneto-thermoelasticity waves with two relaxation times and temperature dependent moduli", *J. Appl. Math. Model.*, **32**(4), 483-500.

Othman, M.I.A. and Lotfy, K. (2009), "Two-dimensional problem of generalized magneto-thermoelasticity with temperature dependent elastic moduli for different theories", *Multi. Model. Mater. Struct.*, **5**(3), 235-242.

Othman, M.I.A. and Atwa, S.Y. (2011), "The effect of magnetic field on 2-D problem of generalized thermo-elasticity without energy dissipation", *Int. J. Ind. Math.*, **3**(3), 213-226.

Othman, M.I.A., Lotfy, K., Said, S.M. and Osman, B. (2012a), “Wave propagation of fiber-reinforced micropolar thermoelastic medium with voids under three theories”, *Int. J. Appl. Math. Mech.*, **8**(12), 52-69.

Othman, M.I.A. and Said, S.M. (2012b), “The effect of mechanical force on generalized thermoelasticity in a fiber-reinforced under three theories”, *Int. J. Thermophys.*, **33**(6), 1082-1099.

Othman, M.I.A., Said, S.M. and Sarker, N. (2013), “Effect of hydrostatic initial stress on a fiber-reinforcedthermoelastic medium with fractional derivative heat transfer”, *Multi. Model. Mater. Struct.*, **9**(3), 410-426.

Othman, M.I.A., Hasona, W.M. and Abd-Elaziz, E.M. (2014), “Effect of rotation on micropolar generalized generalized thermoelasticity with two temperatures using a dual-phase-lag model”, *Can. J. Phys.*, **92**(2), 149-158.

Othman, M.I.A. and Said, S.M. (2015), “The effect of rotation on a fiber-reinforced medium under generalized magneto-thermoelasticity with internal heat source”, *Mech. Adv. Mater. Struct.*, **22**(3), 168-183.

Puri, P. and Jordan, P.M. (2006), “On the propagation of harmonic plane wanes under the two temperature theory”, *Int. J. Eng. Sci.*, **44**(17), 1113-1126.

Quintanilla, R. and Racke, R. (2008), “A note on stability in three-phase-lag heat conduction”, *Int. J. Heat Mass Transf.*, **51**(1-2), 24-29.

Quintanilla, R. (2009), “Spatial behaviour of solutions of the three-phase-lag heat equation”, *Appl. Math. Comput.*, **213**(1), 153-162.

Roy Choudhuri, S.K. (2007), “On a thermoelastic three-phase-lag model”, *J. Therm. Stress.*, **30**, 231-238.

Singh, B. and Singh, S. J. (2004), “Reflection of planes waves at the free surface of a fibre-reinforced elastic half-space”, *Sãdhanã*, **29**(3), 249-257.

Singh, B. (2006), “Wave propagation in thermally conducting linear fibre-reinforced composite materials”, *J. Arch. Appl. Mech.*, **75**(8-9), 513-520.

Tzou, D.Y. (1995), “A unified approach for heat conduction from macro to micro-scales”, *ASME J. Heat Transfer*, **117**(1), 8-16.

Warren, W.E. and Chen, P.J. (1973), “Propagation in the two temperatures theory of thermoelasticity”, *Acta Mechanica*, **16**(1-2), 21-33.

Youssef, H.M. (2005), “Theory of two-temperature generalized thermoelasticity”, *IMA J. Appl. Math.*, **71**(3), 383-390.

Zenkour, A.M. and Abouelregal, A.E. (2015), “The fractional effects of a two-temperature generalized thermoelastic semi-infinite solid induced by pulsed laser heating”, *Arch. Mech.*, **67**(1), 53-73.

CC